Synthesis, Photophysical Properties, and Biomolecular Labeling Studies of Luminescent Platinum(II)-Terpyridyl Alkynyl Complexes

Keith Man-Chung Wong, Wing-Suen Tang, Ben Wai-Kin Chu, Nianyong Zhu, and Vivian Wing-Wah Yam*

Open Laboratory of Chemical Biology of The Institute of Molecular Technology for Drug Discovery and Synthesis, Centre for Carbon-Rich Molecular and Nano-Scale Metal-Based Materials Research, Department of Chemistry, The University of Hong Kong, Pokfulam Road, Hong Kong, People's Republic of China

Received February 7, 2004

Three luminescent alkynylplatinum(II) terpyridyl complexes, [Pt(^{t}Bu$_3$tpy)(C≡C−C$_6$H$_4$−X-4)](OTf) (X = NH$_2$ **1**, NCS **2**, NHCOCH$_2$I **3**), have been synthesized and characterized. Their electrochemical and photophysical properties have been studied, and the molecular structure of **2** has also been determined by X-ray crystallography. Complexes **2** and **3** exhibit strong luminescence in various media, the origin of which has been tentatively assigned as a dπ(Pt) → π*(^{t}Bu$_3$tpy) ^{3}MLCT excited state, with some mixing of a π(C≡CR) → π*(^{t}Bu$_3$tpy) ^{3}LLCT character. Human serum albumin (HSA) has been labeled by the ready reaction of the isothiocyanate and iodoacetamide functional groups in **2** and **3**, to afford the respective bioconjugates, **2-HSA** and **3-HSA**. Both bioconjugates in 50 mM Tris-Cl buffer (pH 7.4) are highly colored and exhibit luminescence in the visible region upon photoexcitation.

Introduction

Organic fluorescent biological labels have been extensively studied due to their use in fluorescence immunoassays,[1] and numerous examples have been developed for biophysical applications and commercial use.[2] Since the short decay lifetime from such fluorescence immunoassays would limit many other biophysical measurements, the search for other luminescent materials with longer lifetimes to serve as biomolecular probes is urged. The accessibility of the use of gated detection by having longer luminescence lifetime can suppress any fluorescence interference from the biological samples. Luminescent transition metal complex systems, which commonly display phosphorescence in the microsecond range, would be ideal candidates in this respect. In addition, longer excitation wavelength, i.e., lower excitation energy, would be anticipated in the process of detection, and thus the degree of photodegradation of biological samples would be minimized. In view of this, establishment of transition metal complexes, such as those containing ruthenium(II),[3] rhenium(I),[4] osmium(II),[5] rhodium(III),[6] and iridium(III),[7] for luminescent biological labeling has been reported. Square-planar platinum(II) complexes, especially those with polypyridyl ligands, have been extensively investigated in view of their rich photoluminescence properties.[8−13] In addition, these complexes have been shown to exhibit interesting spectroscopic and photophysical behaviors associated with the occurrence of Pt···Pt and π···π interactions.[8−10] Apart from the photophysical studies, platinum(II) complexes with square-planar geometry have also attracted considerable attention as a result of their interesting biological activities, such as antitumor cytotoxicity,[14,15] DNA

* Corresponding author. Fax: (852) 2857-1586. E-mail: wwyam@hku.hk.

(1) (a) Hermanson, G. T. *Bioconjugate Techniques*; Academic Press: San Diego, CA, 1996. (b) Kessler, C. *Nonradioactive Labeling and Detection of Biomolecules*, 2nd ed.; Springer: Heidelberg, Germany, 1999. (c) Sammes, P. G.; Yahioglu, G. *Nat. Prod. Rep.* **1996**, *13*, 1.

(2) Haugland, R. P. *Handbook of Fluorescent Probes and Research Chemicals*; Molecular Probes: Eugene, OR, 1996.

(3) (a) Ryan, E. M.; O'Kennedy, R.; Feeney, M. M.; Kelly, J. M.; Vos, J. G. *Bioconjugate Chem.* **1992**, *3*, 285. (b) Youn, H. J.; Terpetschnig, E.; Szmacinski, H.; Lakowicz, J. R. *Anal. Biochem.* **1995**, *232*, 24.

(4) (a) Guo, X. Q.; Castellano, F. N.; Li, L.; Lakowicz, J. R. *Anal. Chem.* **1998**, *70*, 632. (b) Lo, K. K. W.; Ng, D. C. M.; Hui, W. K.; Cheung, K. K. *J. Chem. Soc., Dalton Trans.* **2001**, 2634. (c) Lo, K. K. W.; Hui, W. K.; Ng, D. C. M.; *J. Am. Chem. Soc.* **2002**, *124*, 9344. (d) Lo, K. K. W.; Hui, W. K.; Ng, D. C. M.; Cheung, K. K. *Inorg. Chem.* **2002**, *41*, 40.

(5) Terpetschnig, E.; Szmacinski, H.; Lakowicz, J. R. *Anal. Biochem.* **1996**, *240*, 54.

(6) Lo, K. K. W.; Li, C. K.; Lau, K. W.; Zhu, N. *J. Chem. Soc., Dalton Trans.* **2003**, 4682.

(7) (a) Lo, K. K. W.; Ng, D. C. M.; Chung, C. K. *Organometallics* **2001**, *20*, 4999. (b) Lo, K. K. W.; Ng, D. C. M.; Chung, C. K.; Zhu, N. *New J. Chem.* **2002**, *26*, 81. (c) Lo, K. K. W.; Chung, C. K.; Zhu, N. *Chem. Eur. J.* **2003**, *9*, 475. (d) Lo, K. K. W.; Chung, C. K.; Lee, T. K. M.; Lui, L. H.; Tsang, K. H. K.; Zhu, N. *Inorg. Chem.* **2003**, *42*, 6886.

(8) (a) Miskowski, V. M.; Houlding, V. H. *Inorg. Chem.* **1989**, *28*, 1529. (b) Kunkely, H.; Vogler, A. *J. Am. Chem. Soc.* **1990**, *112*, 5625. (c) Miskowski, V. M.; Houlding, V. H. *Inorg. Chem.* **1991**, *30*, 4446. (d) Houlding, V. H.; Miskowski, V. M. *Coord. Chem. Rev.* **1991**, *111*, 145. (e) Connick, W. B.; Henling, L. M.; Marsh, R. E.; Gray, H. B. *Inorg. Chem.* **1996**, *35*, 6261. (f) Chan, C. W.; Cheng, L. K.; Che, C. M. *Coord. Chem. Rev.* **1994**, *132*, 87.

(9) (a) Yip, H. K.; Che, C. M.; Zhou, Z. Y.; Mak, T. C. W. *J. Chem. Soc., Chem. Commun.* **1992**, 1369. (b) Yip, H. K.; Cheng, L. K.; Cheung, K. K.; Che, C. M. *J. Chem. Soc., Dalton Trans.* **1993**, 2933. (c) Bailey, J. A.; Miskowski, V. M.; Gray, H. B. *Inorg. Chem.* **1993**, *32*, 369. (d) Hill, M. G.; Bailey, J. A.; Miskowski, V. M.; Gray, H. B. *Inorg. Chem.* **1996**, *35*, 4585.

(10) (a) Bailey, J. A.; Hill, M. G.; Marsh, R. E.; Miskowski, V. M.; Schaefer, W. P.; Gray, H. B. *Inorg. Chem.* **1995**, *34*, 4591. (b) Büchner, R.; Cunningham, C. T.; Field, J. S.; Haines, R. J.; McMillin, D. R.; Summerton, G. C. *J. Chem. Soc., Dalton Trans.* **1999**, 711. (c) Tzeng, B. C.; Fu, W. F.; Che, C. M.; Chao, H. Y.; Cheung, K. K.; Peng, S. M. *J. Chem. Soc., Dalton Trans.* **1999**, 1017. (d) Yam, V. W. W.; Wong, K. M. C.; Zhu, N. *J. Am. Chem. Soc.* **2002**, *124*, 6506.

10.1021/om049898h CCC: $27.50
Publication on Web 05/29/2004

Chart 1

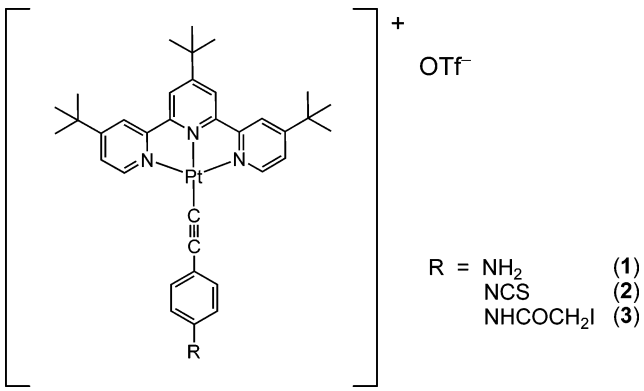

intercalation,[14,16] and protein binding behavior.[17] To our surprise, there has so far been no report on the utilization of this class of platinum(II) complexes as luminescent labeling reagents for biomolecules. Herein we report the synthesis and characterization of three luminescent alkynylplatinum(II) terpyridyl complexes, [Pt(^{t}Bu$_3$tpy)(C≡C−C$_6$H$_4$−X-4)](OTf) (X = NH$_2$ **1**, NCS **2**, NHCOCH$_2$I **3**) (Chart 1). Their electrochemical and photophysical behaviors have been studied, and the molecular structure of **2** has also been determined by X-ray crystallography. In view of the ready reactivity of the isothiocyanate and iodoacetamide functional groups in complexes **2** and **3** with the primary amine and sulfhydryl group, respectively, of biomolecules, human serum albumin (HSA) has been labeled with complexes **2** and **3**. The luminescence properties of the corresponding bioconjugates have been investigated in order to demonstrate their role as potential luminescent labels for biomolecules.

Experimental Section

Materials and Reagents. Dichloro(1,5-cyclooctadiene)-platinum(II) was obtained from Strem Chemicals Inc. 4,4′,4″-Tri-*tert*-butyl-2,2′:6′,2″-terpyridine (^{t}Bu$_3$tpy), thiophosgene (CSCl$_2$), iodoacetic anhydride, and 4-aminophenylacetylene were purchased from Aldrich Chemical Co. [Pt(^{t}Bu$_3$tpy)-(MeCN)](OTf)$_2$[11e,g] was prepared according to literature methods. Human serum albumin (HSA) fraction V was obtained from Calbiochem and was used as received. All buffer components were of molecular biology grade and used without purification. All solvents were purified and distilled using standard procedures before use. All other reagents were of analytical grade and were used as received.

Synthesis. [Pt(^{t}Bu$_3$tpy)(C≡C−C$_6$H$_4$−NH$_2$-4)](OTf) (1). To a stirred solution of 4-aminophenylacetylene (50 mg, 0.43 mmol) in methanol (70 mL) was added sodium hydroxide (23 mg, 0.58 mmol). The resultant solution was stirred at room temperature for 30 min. [Pt(^{t}Bu$_3$tpy)(MeCN)](OTf)$_2$ (300 mg, 0.39 mmol) was added to the reaction mixture and was then heated under reflux for 12 h. The mixture was filtered, and the solvent was evaporated to dryness. The product was isolated by column chromatography on silica gel using dichloromethane−acetone (3:1 v/v) as eluent. Subsequent recrystallization by vapor diffusion of diethyl ether into a dichloromethane solution of the product gave **1** as purple-red crystals. Yield: 200 mg (60%). ^{1}H NMR (400 MHz, (CD$_3$CN), 298 K, relative to Me$_4$Si, δ/ppm): 1.46 (s, 18H, *tert*-butyl protons), 1.54 (s, 9H, *tert*-butyl protons), 4.27 (s, 2H, amino protons), 6.62 (d, 2H, J = 9 Hz, phenyl protons), 7.22 (d, 2H, J = 9 Hz, phenyl protons), 7.72 (dd, 2H, J = 2 Hz, 6 Hz, terpyridyl protons), 8.26 (d, 2H, J = 2 Hz, terpyridyl protons), 8.31 (s, 2H, terpyridyl protons), 9.02 (d with Pt satellite, 2H, J = 6 Hz, J_{Pt-H} = 46 Hz, terpyridyl protons). IR (KBr disk, ν/cm^{-1}): 2112(m) ν(C≡C); 3365(m) ν(N−H). Positive FAB-MS: m/z 712 [M − OTf]$^+$. Anal. Calcd for C$_{36}$H$_{41}$N$_4$F$_3$SO$_3$Pt·1/2CH$_2$Cl$_2$: C, 48.48; H, 4.54; N, 6.20. Found: C, 48.79; H, 4.66; N, 6.20.

[Pt(^{t}Bu$_3$tpy)(C≡C−C$_6$H$_4$−NCS-4)](OTf) (2). To a mixture of **1** (100 mg, 84.4 μmol) and CaCO$_3$ (34 mg, 339.7 μmol) in dry acetone (8 mL) was added CSCl$_2$ (13 μL, 170.5 μmol). After stirring for 2 h in the dark under nitrogen at 0 °C, the suspension was filtered and the filtrate evaporated to dryness to yield an orange-yellow solid. Recrystallization from vapor diffusion of diethyl ether into an acetone solution of the product afforded **2** as orange-yellow crystals. Yield: 60 mg (80%). ^{1}H NMR (400 MHz, (CD$_3$CN), 298 K, relative to Me$_4$Si, δ/ppm): 1.45 (s, 18H, *tert*-butyl protons), 1.53 (s, 9H, *tert*-butyl protons), 7.29 (d, 2H, J = 8 Hz, phenyl protons), 7.47 (d, 2H, J = 8 Hz, phenyl protons), 7.70 (dd, 2H, J = 2 Hz, 6 Hz, terpyridyl protons), 8.27 (d, 2H, J = 2 Hz, terpyridyl protons), 8.31 (s, 2H, terpyridyl protons), 8.96 (d with Pt satellite, 2H, J = 6 Hz, J_{Pt-H} = 43 Hz, terpyridyl protons). IR (KBr disk, ν/cm^{-1}): 2176(m) and 2118(m) ν(NCS). Positive FAB-MS: m/z 754 [M − OTf]$^+$. Anal. Calcd for C$_{37}$H$_{39}$N$_4$F$_3$S$_2$O$_3$Pt: C, 49.17; H, 4.32; N, 6.20. Found: C, 49.09; H, 4.41; N, 6.01.

[Pt(^{t}Bu$_3$tpy)(C≡C−C$_6$H$_4$−NHCOCH$_2$I-4)](OTf) (3). Complex **1** (50 mg, 0.249 mmol) and iodoacetic anhydride (132 mg, 0.373 mmol) were stirred in acetonitrile (8 mL) at room temperature in the dark under an inert atmosphere of nitrogen for 24 h. The solution was evaporated to dryness to give an orange-red solid. The product was purified by column chromatography on silica gel using dichloromethane−acetone (3:1 v/v) as eluent. Subsequent recrystallization by vapor diffusion of diethyl ether into an acetone solution of the product gave **3** as red crystals. Yield: 154 mg (60%). ^{1}H NMR (400 MHz, (CD$_3$CN), 298 K, relative to Me$_4$Si, δ/ppm): 1.46 (s, 18H, *tert*-butyl protons), 1.54 (s, 9H, *tert*-butyl protons), 3.85 (s, 2H, methylene protons), 7.43 (d, 2H, J = 9 Hz, phenyl protons), 7.54 (d, 2H, J = 9 Hz, phenyl protons), 7.72 (dd, 2H, J = 2 Hz, 6 Hz, terpyridyl protons), 8.27 (d, 2H, J = 2 Hz, terpyridyl protons), 8.32 (s, 2H, terpyridyl protons), 8.73 (s, 1H, amide proton), 9.00 (d with Pt satellite, 2H, J = 6 Hz, J_{Pt-H} = 45 Hz, terpyridyl protons). IR (KBr disk, ν/cm^{-1}): 2118(w) ν(C≡C). Positive FAB-MS: m/z 880 [M − OTf]$^+$. Anal. Calcd for

(11) (a) Aldridge, T. K.; Stacy, E. M.; McMillin, D. R. *Inorg. Chem.* **1994**, *33*, 722. (b) Arena, G.; Calogero, G.; Campagna, S.; Scolaro, L. M.; Ricevuto, V.; Romeo, R. *Inorg. Chem.* **1998**, *37*, 2763. (c) Lai, S. W.; Chan, M. C. W.; Cheung, K. K. *Inorg. Chem.* **1999**, *38*, 4267. (d) Yam, V. W. W.; Tang, R. P. L.; Wong, K. M. C.; Ko, C. C.; Cheung, K. K. *Inorg. Chem.* **2001**, *40*, 571. (e) Yam, V. W. W.; Tang, R. P. L.; Wong, K. M. C.; Cheung, K. K. *Organometallics* **2001**, *20*, 4476. (f) McMillin, D. R.; Moore, J. J. *Coord. Chem. Rev.* **2002**, *229*, 113. (g) Yam, V. W. W.; Wong, K. M. C.; Zhu, N. *Angew. Chem., Int. Ed.* **2003**, *42*, 1400.

(12) (a) Zuleta, J. A.; Chesta, C. A.; Eisenberg, R. *J. Am. Chem. Soc.* **1989**, *111*, 8916. (b) Zuleta, J. A.; Burbery, M. S.; Eisenberg, R. *Coord. Chem. Rev.* **1990**, *97*, 47. (c) Paw, W.; Lachicotte, R. J.; Eisenberg, R. *Inorg. Chem.* **1998**, *37*, 4139.

(13) (a) Hissler, M.; Connick, W. B.; Geiger, D. K.; McGarrah, J. E.; Lipa, D.; Lachicotte, R. J.; Eisenberg, R. *Inorg. Chem.* **2000**, *39*, 447. (b) Whittle, C. E.; Weinstein, J. A.; Geore, M. W.; Schanze, K. S. *Inorg. Chem.* **2001**, *40*, 4053. (c) Chan, S. C.; Chan, M. C. W.; Wang, Y.; Che, C. M.; Cheung, K. K.; Zhu, N. *Chem. Eur. J.* **2001**, *7*, 4180. (d) Lu, W.; Chan, M. C. W.; Zhu, N.; Che, C. M.; He, Z.; Wong, K. Y. *Chem. Eur. J.* **2003**, *9*, 6155.

(14) (a) Lippard, S. J. *Acc. Chem. Res.* **1978**, *11*, 211. (b) Che, C. M.; Ma, D. L. *Chem. Eur. J.* **2003**, *9*, 6133.

(15) (a) Rosenberg, B.; Van Camp, L.; Trosko, J. E.; Mansour, V. H. *Nature (London)* **1969**, *222*, 385. (b) McFadyen, W. D.; Wakelin, L. P. G.; Roos, I. A. G.; Leopold, V. A. *J. Med. Chem.* **1985**, *28*, 1113. (c) Fuertes, M. A.; Alonso, C.; Pérez, J. M. *Chem. Rev.* **2003**, *103*, 645.

(16) (a) Jamieson, E. R.; Lippard, S. J. *Chem. Rev.* **1999**, *99*, 2467. (b) Peyratout, C. S.; Aldridge, T. K.; Crites, D. K.; McMillin, D. R. *Inorg. Chem.* **1995**, *34*, 4484. (c) Che, C. M.; Yang, M.; Wong, K. H.; Chan, H. L.; Lam, W. *Chem. Eur. J.* **1999**, *5*, 3350.

(17) Ratilla, E. M. A.; Brothers, H. M.; Kostić, N. M. *J. Am. Chem. Soc.* **1987**, *109*, 4592.

$C_{38}H_{42}N_4SO_5F_3IPt\cdot(CH_3)_2CO$: C, 44.61; H, 4.35; N, 5.08. Found: C, 44.86; H, 4.27; N, 5.33.

Labeling of Biomolecules. Labeling of Human Serum Albumin (HSA) with Complex 2. Complex **2** (1.3 mg, 1.67 μmol) in 20 μL of anhydrous DMSO was added to HSA (1.32 mg, 20 nmol) in 50 mM carbonate buffer (pH 9.0). The mixture was incubated in the dark at 25 °C for 12 h. The solid residue was removed by centrifugation. The supernatant was diluted to 1 mL with 50 mM Tris-HCl (pH 7.4) and loaded onto a PD-10 column (Pharmacia) that had been equilibrated with the same buffer. The first band eluted out of the column with an intense red color was collected, and the solution was concentrated with a YM-50 centricon (Amicon). The labeled protein was further purified by HPLC equipped with a size-exclusion column. The mobile phase was 50 mM Tris-HCl (pH 7.4) at a flow rate of 1 mL min^{-1}.

Labeling of Human Serum Albumin (HSA) with Complex 3. The procedure was similar to that described for the labeling of HSA with complex **2** except that 50 mM potassium phosphate buffer (pH 7.0) was used instead.

Physical Measurements and Instrumentation. The ^{1}H NMR spectra were recorded on a Bruker DPX-400 FT-NMR spectrometer (400 MHz) in CD_3CN at 298 K with chemical shifts reported relative to Me_4Si. Positive-ion FAB-mass spectra were recorded on a Finnigan MAT95 mass spectrometer. The UV/vis spectra were obtained on a Hewlett-Packard 8452A diode array spectrophotometer and IR spectra as KBr disks on a Bio-Rad FTS-7 Fourier transform infrared spectrophotometer (4000−400 cm^{-1}). Elemental analyses of the new complexes were performed on a Carlo Erba 1106 elemental analyzer at the Institute of Chemistry, Chinese Academy of Sciences. Steady-state excitation and emission spectra were obtained on a Spex Fluorolog 111 spectrofluorometer. Solid-state photophysical studies were carried out with solid samples contained in a quartz tube inside a quartz-walled Dewar flask. Measurements of solid samples at 77 K were conducted using a liquid nitrogen-filled optical Dewar flask. Excited-state lifetimes of solution samples were measured using a conventional laser system. The excitation source used was the 355 nm output (third harmonic, 8 ns) of a Spectra-Physics Quanta-Ray Q-switched GCR-150 pulsed Nd:YAG laser (10 Hz). Luminescence quantum yields were measured by the optical dilute method reported by Demas and Crosby.[18] A degassed aqueous solution of $[Ru(bpy)_3]Cl_2$ (ϕ = 0.042, excitation wavelength at 436 nm) was used as the reference.[19] All solutions for photophysical studies were degassed on a high-vacuum line in a two-compartment cell consisting of a 10 mL Pyrex bulb and a 1 cm path length quartz cuvette and sealed from the atmosphere by a Bibby Rotaflo HP6 Teflon stopper. The solutions were subject to no less than four freeze−pump−thaw cycles. Cyclic voltammetric measurements were performed by using a CH Instruments, Inc. model CHI 600A electrochemical analyzer. The electrolytic cell used was a conventional two-compartment cell. Electrochemical measurements were performed in acetonitrile solutions with 0.1 M $^nBu_4NPF_6$ (TBAH) as supporting electrolyte at room temperature. The reference electrode was a $Ag/AgNO_3$ (0.1 M in acetonitrile) electrode, and the working electrode was a glassy carbon electrode (CH Instruments, Inc.) with a platinum wire as the counter electrode. The working electrode surface was first polished with 1 mm alumina slurry (Linde) on a microcloth (Buehler Co.). It was then rinsed with ultrapure deionized water and sonicated in a beaker containing ultrapure water for 5 min. The polishing and sonicating steps were repeated twice, and then the working electrode was finally rinsed under a stream of ultrapure deionized water. The ferrocenium/ferrocene couple ($FeCp_2^{+/0}$) was used as the internal reference. All solutions for electrochemical studies were deaerated with prepurified argon gas just before measurements.

(18) Demas, J. N.; Crosby. G. A. *J. Phys. Chem.* **1971**, *75*, 991.
(19) van Houten, J.; Watts, R. *J. Am. Chem. Soc.* **1976**, *98*, 4853.

Table 1. Crystallographic and Structural Refinement Data for Complex 2

empirical formula	$C_{37}H_{39}F_3N_4O_3PtS_2$
fw	903.93
temperature	301(2) K
wavelength	0.71073 Å
cryst syst	monoclinic
space group	*C*2/*c*
unit cell dimens	a = 32.053(6) Å, b = 10.973(2) Å, c = 21.495(4) Å; β = 95.03(3)°
volume	7531(2) Å^3
Z	8
density (calcd)	1.594 g cm^{-3}
abs coeff	3.893 mm^{-1}
F(000)	3600
cryst size	0.30 × 0.30 × 0.15 mm
data collection range	1.96 to 25.35°
index ranges	$-38 \le h \le 38$, $-13 \le k \le 13$, $-23 \le l \le 23$
no. of reflns collected	22 215
no. of indep reflns	6509 [R(int)[a] = 0.0397]
completeness to θ = 25.35°	94.3%
absorp corr	none
refinement method	full-matrix least-squares on F^2
no. of data/restraints/params	6509/0/436
goodness-of-fit[b] on F^2	1.011
final R indices [$I>2\sigma(I)$][c]	R1 = 0.0349, wR2 = 0.0934
R indices (all data)	R1 = 0.0440, wR2 = 0.0988
largest diff peak and hole	0.975 and −1.726 e Å^{-3}

[a] $R_{int} = \sum|F_o^2 - F_o^2(\text{mean})|/\sum[F_o^2]$. [b] GooF = $\{\sum[w(F_o^2 - F_c^2)^2]/(n-p)\}^{1/2}$, where n is the number of reflections and p is the total number of parameters refined. The weighting scheme is $w = 1/[\sigma^2(F_o^2) + (aP)^2 + bP]$, where P is $[2F_c^2 + \text{Max}(F_o^2,0)]/3$. [c] R1 = $\sum||F_o| - |F_c||/\sum|F_o|$, wR2 = $\{\sum[w(F_o^2 - F_c^2)^2]/\sum[w(F_c^2)^2]\}^{1/2}$.

X-ray Crystal Structure Determination. Single crystals of **2** were obtained by vapor diffusion of diethyl ether into an acetone solution of the complex. A crystal of dimensions 0.30 × 0.30 × 0.15 mm mounted in a glass capillary was used for data collection at 301 K on a MAR diffractometer with a 300 mm image plate detector using graphite-monochromatized Mo Kα radiation (λ = 0.71073 Å). Data collection was made with 2° oscillation of φ steps, 8 min exposure time, and a scanner distance of 120 mm. A total of 82 images were collected. The images were interpreted and intensities integrated using DENZO.[20] The structure was solved by direct methods employing SIR-97.[21] The Pt and S atoms and most of the non-hydrogen atoms were located according to direct methods and successive least-squares Fourier cycles. The positions of other non-hydrogen atoms were found after successful refinement by full-matrix least-squares using SHELXL 97.[22] All 6509 independent reflections (R_{int} equal to 0.0397, 5153 reflections larger than $4\sigma(F_o)$) from a total 22 215 reflections participated in the full-matrix least-squares refinement against F^2, where $R_{int} = \sum|F_o^2 - F_o^2(\text{mean})|/\sum[F_o^2]$. These reflections were in the range $-38 \le h \le 38$, $-13 \le k \le 13$, $-23 \le l \le 23$ with $2\theta_{max}$ equal to 50.70°. One crystallographic asymmetric unit consists of one formula unit. Hydrogen atoms were generated using SHELXL 97 and their positions calculated based on the riding mode with thermal parameters equal to 1.2 times that of associated C atoms and participated in the calculation of the

(20) Written with the cooperation of the program authors Otwinowski, Z.; Minor, W.; Gewirth, D. *DENZO: The HKL Manuals A description of programs DENZO, XDISPLAYF, and SCALEPACK*; Yale University: New Haven, 1995.
(21) Sir97: a new tool for crystal structure determination and refinement: Altomare, A.; Burla, M. C.; Camalli, M.; Cascarano, G.; Giacovazzo, C.; Guagliardi, A.; Moliterni, A. G. G.; Polidori, G.; Spagna, R. *J. Appl. Crystallogr.* **1998**, *32*, 115.
(22) SHELXL97: Sheldrick, G. M. *SHELXL97: Programs for Crystal Structure Analysis (release 97-2)*; University of Göttingen: Göttingen, Germany, 1997.
(23) (a) Blanton, C. B.; Murtaza, Z.; Shaver, R. J.; Rillema, D. P. *Inorg. Chem.* **1992**, *31*, 3230. (b) von Zelewsky, A.; Gremaud, G. *Helv. Chim. Acta* **1988**, *84*, 85.

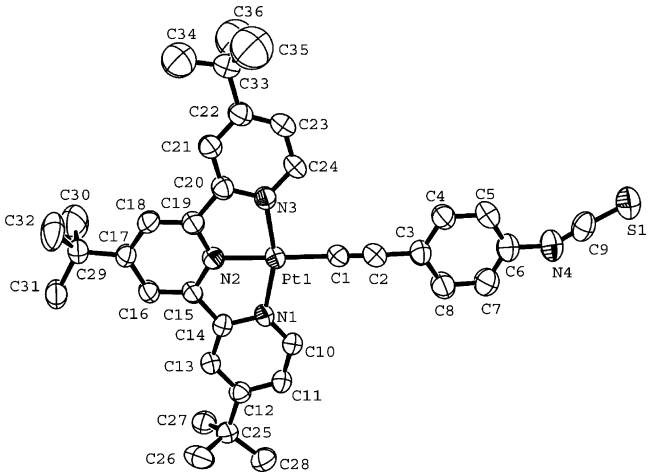

Figure 1. Perspective drawing of the complex cation of **2** with atomic numbering scheme. Hydrogen atoms are omitted for clarity. Thermal ellipsoids are drawn at 50% probability level.

final *R*-indices. Convergence ($(\Delta/\sigma)_{max} = 0.001$, av 0.001) for 436 variable parameters by full-matrix least-squares refinement on F^2 reaches $R_1 = 0.0349$ and $wR_2 = 0.0934$ with a goodness-of-fit of 1.011. Crystallographic and structural refinement data are given in Table 1.

Results and Discussion

Synthesis and Characterization. Complex **1** was prepared according to modification of a previously reported procedure,[11e,g] involving the reaction of [Pt(^{t}Bu$_3$tpy)(MeCN)](OTf)$_2$ with 4-aminophenylacetylene in the presence of sodium hydroxide in methanol under reflux conditions. Complexes **2** and **3** were synthesized from the reaction of complex **1** with $SCCl_2$ and iodoacetic anhydride, respectively, in acetone. The presence of three *tert*-butyl groups on the terpyridyl ligand allows for purification by column chromatography on silica gel, and the dark purple band containing **1** and the orange band containing **3** were collected as the desired products. The identities of complexes **1**−**3** have been confirmed by ^{1}H NMR spectroscopy, FAB-mass spectrometry, IR spectroscopy, and satisfactory elemental analyses. The crystal structure of **2** has also been determined by X-ray crystallography. The IR spectra of **1** and **3** show a weak band at 2112 and 2118 cm^{-1}, respectively, typical of the ν(C≡C) stretching frequency. Due to the relatively weak intensity of this stretch together with the overlapping of the much more intense ν(N═C═S) stretch located at a similar frequency in complex **2**, no attempts were made to assign the ν(C≡C) stretch in **2**. In the NMR spectra, the electron-withdrawing effects of the carbonyl group in **3** resulted in the downfield shift of the amide NH signal (δ 8.37 ppm) compared to the corresponding NH_2 signal of **1** (δ 4.27 ppm).

Crystal Structure Determination. The perspective drawing of the complex cation of **2** is shown in Figure 1. Selected bond distances and bond angles are tabulated in Table 2. The platinum(II) center, coordinated to a terpyridyl and an alkynyl group, adopts a distorted square-planar geometry. Due to the steric demand of the terpyridyl ligand, the N−Pt−N angles [N(1)−Pt(1)−N(2) 80.89°; N(2)−Pt(1)−N(3) 80.24°; N(1)−Pt(1)−N(3) 161.03°] show deviations from the idealized values of

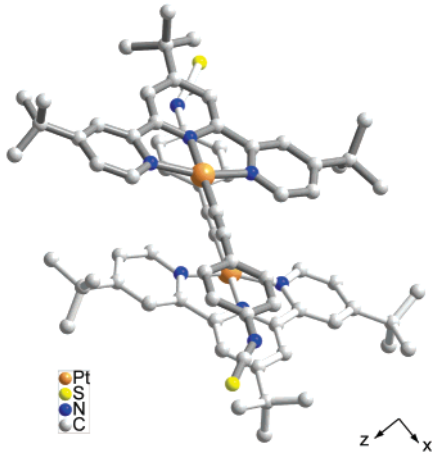

Figure 2. Ball-and-stick model showing the head-to-tail arrangement of two complex cations of **2**, from the view along the *y*-axis.

Table 2. Selected Bond Distances (Å) and Bond Angles (deg) for Complex 2 with Estimated Standard Deviations (esds) Given in Parentheses

Pt(1)−N(1)	2.012(4)	Pt(1)−N(2)	1.947(4)
Pt(1)−N(3)	2.007(4)	Pt(1)−C(1)	1.988(5)
C(1)−C(2)	1.154(7)	C(2)−C(3)	1.454(8)
N(4)−C(6)	1.395(7)	N(4)−C(9)	1.167(7)
S(1)−C(9)	1.573(7)		
N(1)−Pt(1)−N(2)	80.89(15)	N(2)−Pt(1)−N(3)	80.24(16)
C(1)−Pt(1)−N(3)	99.19(18)	C(1)−Pt(1)−N(1)	99.63(17)
N(1)−Pt(1)−N(3)	161.03(16)	N(2)−Pt(1)−C(1)	178.68(18)
Pt(1)−C(1)−C(2)	179.2(5)	C(1)−C(2)−C(3)	177.6(6)
C(6)−N(4)−C(9)	147.9(7)	N(4)−C(9)−S(1)	175.6(6)

90° and 180°. Similar to a related platinum-terpyridyl complex, [Pt(tpy)(C≡C−C$_6$H$_5$)]$^+$,[11e] the small dihedral angle (4.06°) between the platinum-terpyridyl plane and the phenyl group of the alkynyl ligand indicates an essentially coplanar arrangement of these two planes. The isothiocyanate functional group shows a linear arrangement about N(4)−C(9)−S(1) with a bond angle of 175.6° and an exceptionally large C(6)−N(4)−C(9) bond angle of 147.9°, which are commonly observed in a related transition metal isothiocyanato system.[4b] As a result of sp hybridization of the alkynyl carbon atoms, an essentially linear arrangement about the alkynyl group [Pt(1)−C(1)−C(2) 179.2°; C(1)−C(2)−C(3) 177.6°] is observed. The bond lengths of Pt−N [Pt(1)−N(1) 2.012 Å; Pt(1)−N(2) 1.947 Å; Pt(1)−N(3) 2.007 Å] are comparable to that of other platinum(II)-terpyridyl systems,[9a,b,10,11a,c−e,g] while the Pt(1)−C(1) bond of 1.988 Å and C(1)−C(2) of 1.154 Å are in the range typical of platinum(II)-alkynyl complexes.[10d,11e,g,13a,c,d] It is interesting to note that two nearby complex cations show a head-to-tail conformation with a Pt···Pt distance of 4.033 Å, as shown in Figure 2, to minimize the mutual repulsion between the sterically bulky tri-*tert*-butylterpyridine ligands despite the fact that no significant Pt···Pt or π···π interactions are observed.

Electrochemistry. The cyclic voltammograms of complexes **1**−**3** in acetonitrile (0.1 M ^{n}Bu$_4$NPF$_6$) show two quasi-reversible reductions at −1.00 and −1.5 V (vs SCE) and one irreversible oxidation at +0.71 to +1.41 V. Their electrochemical data are tabulated in Table 3. The two reduction couples, which are independent of the nature of substituents on the alkynyl ligand, are assigned as the two successive reductions of the ter-

Table 3. Electrochemical Data for 1−3[a]

complex	oxidation E_{pa}/V vs SCE[b]	reduction $E_{1/2}$/V vs SCE[c] (ΔE_p/mV)
1	+0.71	−1.02 (82)
		−1.52 (64)
2	+1.41	−0.99 (75)
		−1.46 (72)
3	+0.93	−1.00 (52)
		−1.50 (54)

[a] In acetonitrile solution with 0.1 M $^nBu_4NPF_6$ (TBAH) as supporting electrolyte at room temperature; scan rate 100 mV s^{-1}. [b] E_{pa} refers to the anodic peak potential for the irreversible oxidation waves. [c] $E_{1/2} = (E_{pa} + E_{pc})/2$; E_{pa} and E_{pc} are peak anodic and peak cathodic potentials, respectively.

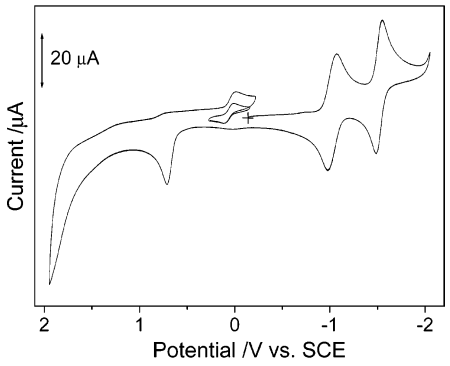

Figure 3. Cyclic voltammogram of complex **2**.

pyridyl ligand. Similar observations have been reported and similar assignments have also been made for other related platinum(II)-terpyridyl systems.[10d,11d] The presence of three electron-donating *tert*-butyl groups on the terpyridyl ligand did not seem to cause a significant shift in the reduction potentials of complexes **1**−**3** relative to that of the unsubstituted terpyridyl analogue, $[Pt(tpy)(C{\equiv}C-R)]^+$.[11d] In general, the oxidation wave was found to occur at more positive potential for the complexes with less electron-rich alkynyl ligands, such that **2** (+1.41 V) > **3** (+0.93 V) > **1** (+0.71 V), in line with the electron-richness of the substituent on the alkynyl ligand, NCS < $NHCOCH_2I$ < NH_2, resulting in the energy of the dπ(Pt) orbital in the order **2** < **3** < **1**. With reference to previous electrochemical studies of related platinum(II) complexes,[11d,13a,d,24] the irreversible oxidation wave is ascribed to a Pt(II) to Pt(III) oxidation process. Similar trends have also been reported in other related alkynylplatinum(II)-terpyridyl complexes.[11d] It is interesting to note that an additional quasi-reversible redox couple appeared at ca. +0.06 V in **1** upon reverse scanning toward cathodic potential after passing through the irreversible oxidation wave, as shown in Figure 3. In view of the fact that such a phenomenon is observed only in complex **1**, the additional quasi-reversible couple resulting from an EC mechanism is suggested to be derived from the decomposed products generated from the irreversible oxidation of the amino group in **1**.

UV−Vis Absorption. The electronic absorption spectra of complexes **1**−**3** in acetonitrile solution display high-energy absorption bands at 246−340 nm and low-energy absorption bands at 400−488 nm. Table 4 summarizes their photophysical data, and Figure 4 shows the electronic absorption spectra of complexes **1**−**3** in acetonitrile solution at 298 K. In view of the similar absorption bands observed in other platinum(II)-terpyridyl systems,[9−11] the intense vibronic-structured high-energy absorption bands, with extinction coefficients (ϵ) on the order of 10^4 dm^3 mol^{-1} cm^{-1}, are assigned as intraligand (IL) $\pi \rightarrow \pi^*(^tBu_3\text{-tpy})$ transition of the terpyridyl ligand. With reference to previous spectroscopic work on related complexes, $[\{Pt(^tBu_3tpy)\}_2(C{\equiv}C)_n]^{2+}$ (n = 1, 2, and 4) and $[Pt(tpy)(C{\equiv}CR)]^+$,[10d,11d,g] the less intense low-energy absorption bands, with extinction coefficients (ϵ) on the order of 10^3 dm^3 mol^{-1} cm^{-1}, are assigned to dπ(Pt) → $\pi^*(^tBu_3tpy)$ metal-to-ligand charge transfer (MLCT) transition, probably with some mixing of $\pi(C{\equiv}CR) \rightarrow \pi^*(^tBu_3tpy)$ ligand-to-ligand charge transfer (LLCT) transition, supported by electrochemical studies. The different solution colors of the complexes observed in acetonitrile (purple-blue in **1**, yellow in **2**, and orange-red in **3**) parallel the occurrence of low-energy absorption bands at different wavelengths, with **1** at 488 nm, **2** at 424 nm, and **3** at 448 nm (Figure 4). The energy trend of these absorption bands, **1** < **3** < **2**, follows the degree of electron-richness of the substituent group on the alkynyl ligand, NH_2 > $NHCOCH_2I$ > NCS. Complex **1** with an amino group absorbs at the lowest energy, while **2** with an isothiocyanate group absorbs at the highest energy, in accordance with the MLCT/LLCT admixture assignment of the low-energy absorption band. The electron-donating NH_2 group is the most electron-rich alkynyl ligand and hence will raise the dπ(Pt) orbital energy to the largest extent in **1**. As a result, the HOMO−LUMO energy gap of the MLCT transition would be the smallest in **1**, assuming the $\pi^*(^tBu_3tpy)$ energy is insignificantly perturbed. On the other hand, the electron-withdrawing isothiocyanate group in **2** causes the dπ(Pt) orbital to be the lowest lying in energy, giving rise to the highest MLCT transition energy.

Photoluminescence. Upon photoexcitation, complexes **2** and **3** display intense emission bands at ca. 560−643 nm in fluid solution and in the solid state at 298 K and at 77 K, while complex **1** is only emissive at 77 K in glass medium. The photophysical data are collected in Table 4. The large Stoke's shift together with the relatively long emission lifetime in the microsecond range suggest that the emission originates from a spin-forbidden triplet excited state. With reference to previous spectroscopic studies on related complexes, $[\{Pt(^tBu_3tpy)\}_2(C{\equiv}C)_n]^{2+}$ (n = 1, 2, and 4) and $[Pt(tpy)(C{\equiv}CR)]^+$,[10d,11d,g] together with consideration of the close resemblance of the excitation band at ca. 433−460 nm to the low-energy electronic absorption band at ca. 440 nm in **2** and **3**, an emission origin of a dπ(Pt) → $\pi^*(^tBu_3tpy)$ ^{3}MLCT excited state, with some mixing of a $\pi(C{\equiv}CR) \rightarrow \pi^*(^tBu_3tpy)$ ^{3}LLCT state, is tentatively assigned. Figure 5 displays the excitation and emission spectra of **2** and **3** in acetonitrile solution at 298 K. Similar to the electronic absorption study, the observation of the emission band of **2** at higher energy than that of **3** is in line with the lower electron-richness of the isothiocyanate group than the iodoacetamide, which would lower the dπ(Pt) orbital energy in **2**, causing a higher energy MLCT emission. The nonemissive behavior of **1** in the solid state and in acetonitrile solution may be ascribed to the quenching by photoinduced electron transfer (PET), in which the electron is transferred from the electron-rich amino group to the platinum metal center to quench the emissive ^{3}MLCT excited

Table 4. Photophysical Data for Complexes 1−3 and Bioconjugates 2-HSA and 3-HSA

complex or bioconjugate	medium (T [K])	absorption λ_{max}/nm (ϵ_{max}/dm^3 mol^{-1} cm^{-1})	emission λ_{max}/nm (τ_o/μs)	Φ_{lum}
1	MeCN (298)	254 (42 680), 272 (47 310), 286 (53 935), 310 (23 515), 326 (19 220), 338 (16 935), 400 (3930), 488 (4920)	nonemissive	
	solid (298)		nonemissive	
	solid (77)		nonemissive	
	^{n}PrCN (77)		590 (9.41) and 708[a] (1.55)	
2	MeCN (298)	246 (44 520), 270 (37 920), 286 (46 300), 298 (51 620), 316 (53 340), 338 (22 610), 400 (7560), 424 (8305)	586 (0.56)	0.019
	solid (298)		583 (0.48)	
	solid (77)		560, 600(6.40)	
	^{n}PrCN (77)		522 (14.71), 630[a] (2.59)	
3	MeCN (298)	250 (50 290), 270 (46 650), 286 (51 580), 308 (40 010), 326 (28 100), 340 (23 220), 404 (5960), 448 (7070)	638 (0.49)	7.2×10^{-4}
	solid (298)		638 (0.15)	
	solid (77)		643 (1.65)	
	^{n}PrCN (77)		550 (13.3), 626[a] (2.71)	
2-HSA	buffer[b] (298)	288, 320, 470	650	5.3×10^{-4}
3-HSA	buffer[b] (298)	280, 334, 466	630	0.013

[a] Excitation wavelength > 540 nm. [b] 50 mM Tris-Cl buffer (pH 7.4).

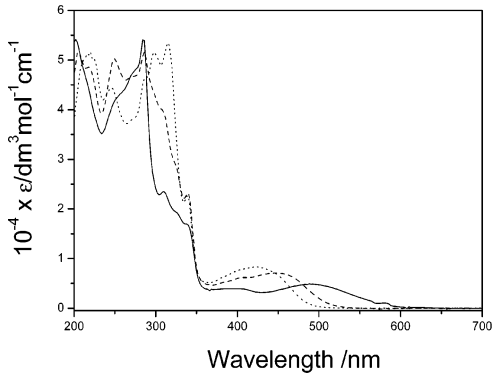

Figure 4. Electronic absorption spectra of **1** (—), **2** (···), and **3** (- - -) in acetonitrile solution at 298 K.

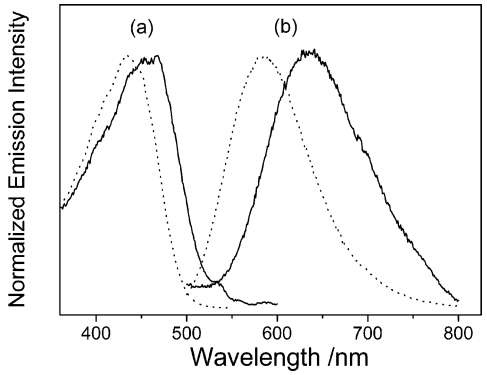

Figure 5. Excitation (a) and emission (b) spectra of **2** (—) and **3** (···) in acetonitrile at 298 K.

state. Alternatively, the quenching of the ^{3}MLCT excited state may be attributed to the presence of an energetically accessible or lower-lying ^{3}LLCT excited state, as a result of a relatively higher-lying π(C≡CR) orbital due to the presence of the electron-donating amino substituent. Other related complexes, such as [Pt(tpy)(C≡C−C_6H_4−OMe)]$^{+}$[11d] or [Pt(bpy)(C≡C−C_6H_4−OMe)$_2$],[13a] bearing electron-donating substituents were reported to be nonemissive or weakly emissive. It is noteworthy that complexes **1**−**3** in 77 K glass display dual luminescence, with a vibronic-structured high-energy emission band

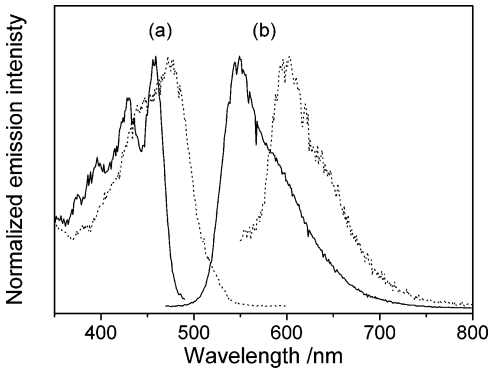

Figure 6. Excitation spectra (a) monitored at 520 nm (—) and at 630 nm (···) and emission spectra (b) upon excitation at 440 nm (—) and 520 nm (···) of **3** in butyronitrile glass at 77 K.

at 522−590 nm and a low-energy one at 626−708 nm (Figure 6). In view of the large differences in the excited-state lifetimes and the excitation spectra derived from these two emission bands, they are suggested to be of different origins. The high-energy emission band with vibrational progressional spacings of ca. 1215 cm^{-1} is assigned as intraligand phosphorescence of the terpyridyl ligand, while the low-energy emission band is assigned to be derived from the ^{3}MLCT/^{3}LLCT phosphorescence.

Labeling of Biomolecule. In view of the ready reaction of the isothiocyanate and the iodoacetamide groups with the respective primary amine and sulfhydryl groups of biomolecules, complexes **2** and **3** are designed to act as luminescent biolabeling agents via the formation of a thiourea and thioether linkage, respectively. In this report, the protein human serum albumin (HSA) has been labeled with complexes **2** and **3** to afford the bioconjugates **2-HSA** and **3-HSA** (Scheme 1), respectively, and purified by size-exclusion chromatography to remove any unreacted complexes. The bioconjugates **2-HSA** and **3-HSA** display a low-energy absorption band at 470 and 462 nm, respectively, in their electronic absorption spectra, indicating the successful attachment of the [Pt(^{t}Bu$_3$tpy)(C≡C−R)]$^+$ moiety

Scheme 1

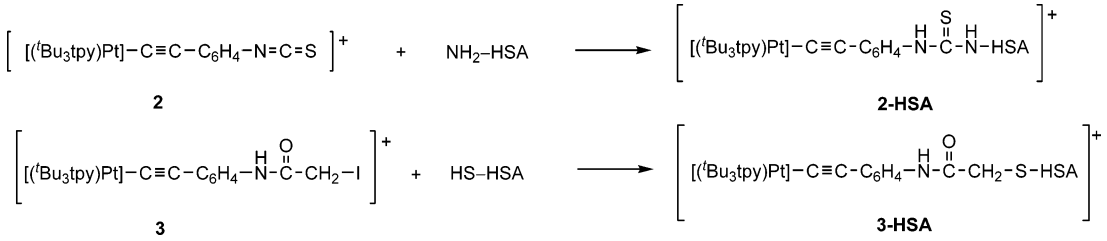

onto the protein. The low-energy absorptions of the bioconjugates are characteristic of the alkynyl platinum(II)-terpyridyl moiety and are attributed to an MLCT/LLCT admixture. Such absorptions are slightly red-shifted with respect to the parent complexes **2** and **3**, probably as a result of the perturbation associated with the electronic as well as environmental effects of the protein and the solution media. Upon photoexcitation, the bioconjugates **2-HSA** and **3-HSA** in 50 mM Tris-Cl buffer (pH 7.4) exhibit an emission band at 650 and 630 nm, respectively (Figure 7). Despite different medium conditions, it is interesting to note that the emission energy of **2-HSA** (650 nm in buffer solution) is much lower than that of its parent complex **2** (586 nm in acetonitrile), while similar emission energy is observed for **3-HSA** (630 nm in buffer solution) and **3** (638 nm in acetonitrile). On the basis of the spectroscopic studies of complexes **2** and **3**, the emission origin of **2-HSA** and **3-HSA** are assigned as derived from a dπ(Pt) → π^*(^{t}Bu$_3$tpy) ^{3}MLCT excited state, with some mixing of a π(C≡CR) → π^*(^{t}Bu$_3$tpy) ^{3}LLCT state. The change in emission energy from **2** to **2-HSA** is attributed to the decrease in electron-withdrawing ability of the thiourea group with respect to the isothiocyanate group, giving rise to a higher dπ(Pt) orbital energy in **2-HSA** and hence a lower MLCT emission energy. The phenomenon of the bioconjugate and its label exhibiting different emission colors is quite unusual since very similar emission energy is usually observed for the bioconjugate and its label in other transition metal luminescent biological labeling systems.[3a,b,4b,d,5,7a,b,d] The higher emission energy observed in the bioconjugate **3-HSA** relative to **2-HSA** (Figure 7) is attributed to the higher electron-withdrawing ability of the amide functionality in **3-HSA** than the thiourea group in **2-HSA**. The excited-state lifetimes of both **2-HSA** and **3-HSA** in buffer solution are in the submicrosecond range (<0.1 μs) and cannot be determined with certainty with our equipment. The higher luminescence quantum yield, Φ_{lum}, of **3-HSA** (0.013) than **2-HSA** (5.3×10^{-4}) suggests that complex **3** could act as a potential luminescent biolabeling agent owing to its higher emission intensity. Despite a low luminescence quantum yield for **2-HSA**, the ability of the bioconjugate to emit with a different color from its parent complex may find interesting applications in luminescent biolabeling.

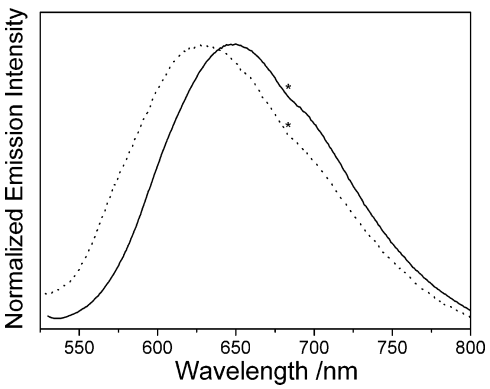

Figure 7. Emission spectra of **2-HSA** (—) and **3-HSA** (···) in 50 mM Tris-Cl (pH 7.4) buffer solution at 298 K. The asterisk denotes the instrumental artifact.

Concluding Remarks

A series of alkynylplatinum(II)-terpyridyl complexes, [Pt(^{t}Bu$_3$tpy)(C≡C−C$_6$H$_4$−X-4)](OTf) (X = NH$_2$, NCS, and NHCOCH$_2$I), have been synthesized and characterized. The X-ray crystal structure of [Pt(^{t}Bu$_3$tpy)(C≡C−C$_6$H$_4$−NCS-4)](OTf) has been determined. Electrochemical studies show that all the complexes display two quasi-reversible reduction couples and one irreversible oxidation wave in the cyclic voltammograms, corresponding to the successive reduction of the terpyridine ligand and a Pt(II) → Pt(III) metal-centered oxidation, respectively. A low-energy absorption band at 400−488 nm is observed in their electronic absorption spectra, assignable to a dπ(Pt) → π^*(^{t}Bu$_3$tpy) MLCT transition, mixed with a π(C≡CR) → π^*(^{t}Bu$_3$tpy) LLCT transition. Upon photoexcitation, intense emission bands at 586−708 nm are observed, which are believed to originate from the excited states of ^{3}MLCT/^{3}LLCT character. The complexes [Pt(^{t}Bu$_3$-tpy)(C≡C−C$_6$H$_4$−NCS-4)](OTf) and [Pt(^{t}Bu$_3$-tpy)(C≡C−C$_6$H$_4$−NHCOCH$_2$I-4)](OTf) are designed to be utilized as luminescent labels, and human serum albumin (HSA) has been labeled with these two complexes to afford the corresponding bioconjugates. Similar to their parent labels, both bioconjugates are highly colored and exhibit luminescence in the visible region upon photoexcitation. The bioconjugate resulting from the isothiocyanate complex is found to emit with a different luminescence color when compared to its parent label, while the bioconjugate derived from the iodoacetamide complex is found to emit with a higher luminescence intensity.

Acknowledgment. V.W.-W.Y. acknowledges support from the University Grants Committee Area of Excellence Scheme and The University of Hong Kong Foundation for Educational Development and Research Limited. B.W.-K.C. acknowledges the receipt of a University Postdoctoral Fellowship and W.-S.T. the receipt of a postgraduate studentship, both administered by The University of Hong Kong. Helpful discussions and assistance provided by Dr. Kenneth K.-W. Lo are gratefully acknowledged.

Supporting Information Available: Tables giving atomic coordinates, anisotropic thermal parameters, bond lengths, and bond angles for complex **2**. This material is available free of charge via the Internet at http://pubs.acs.org.

OM049898H